A recurrent neural network for l_1 anisotropic viscoelastic full waveform inversion with high-order total variation regularization

Tianze Zhang[1], Jian Sun[2], Kristopher Innanen[1], Daniel Trad[1]
[1]University of Calgary [2]The Pennsylvania State University

Summary

A theory-guided deep learning approach to full waveform inversion has features which make it increasingly relevant as we treat problems of greater and greater complexity (e.g., when number of parameter classes increases). Here, we design a recurrent neural network (RNN) for anisotropic viscoelastic full waveform inversion. Eight parameters are simultaneously inverted for, the elastic parameters C_{11} , C_{13} , C_{33} , C_{44} , and their corresponding attenuation parameters QC_{11}, QC_{13}, QC_{33}, QC_{44}, The RNN is built around the velocity-stress anisotropic viscoelastic wave equation. It is a convenient environment in which to compute medium property FWI updates, given a non self-adjoint wave operator, and when the objective function is not analytically differentiable.

Introduction

Our formulation involves a deep learning recurrent neural network, designed in accordance with the velocity-stress equations for anisotropic-viscoelastic wave propagation. Within such a framework the inversion gradient for the parameters in complex media with the complex objective functions can be conveniently calculated. However, to select some of the details of the optimization approach first requires some experimentation, especially in the context of simultaneous recovery of large numbers of model parameters and parameter classes. In this abstract, first, we summarize the design of the RNN for simulation of viscoelastic-anisotropic wave propagation and inversion. Second, we discuss the numerical response an optimization based on $\boldsymbol{l_1}$ measure of misfit, coupled with a high-order TV regularization. Third, we exemplify the approach with synthetic examples.

Theory

We begin by setting out the equations of wave propagation used in the network. The constitutive relationship for a viscoelastic media is (Christensen, 2012; Fan et al., 2016) :

$$\sigma_{ij} = C_{ijkl} \otimes \dot{\varepsilon_{kl}} = \dot{C_{ijkl}} \otimes \varepsilon_{kl}, \tag{1}$$

where the elements C_{ijkl} are the relaxation-stiffness matrix parameters, $\otimes$ denotes time domain convolution, the dot denotes time differentiation, and σ_{ij} and ε_{kl} are the stress and strain tensors respectively. Within the General Standard Linear Solid (GSLS) model, each element of C_{ijkl} has the form:

$$
\dot{\boldsymbol{C}} = \begin{bmatrix} \dot{C_{11}} & \dot{C_{13}} & 0 \\ \dot{C_{13}} & \dot{C_{33}} & 0 \\ 0 & 0 & \dot{C_{44}} \end{bmatrix}. \tag{2}
$$

The corresponding attenuation model can be expressed as:

$$
\mathbf{QC} = \begin{bmatrix} QC_{11} & QC_{13} & 0 \\ QC_{13} & QC_{33} & 0 \\ 0 & 0 & QC_{44} \end{bmatrix}. \tag{3}
$$

In this test we use the one layer of relaxation time for GSLS. The relaxation time between the stress and strain with quality parameter Q can be found in Fathalian, A. (2019). In our RNN, the discretized solution of these equations largely follows Robertson et al. (1994), with the partial derivatives, calculated using the staggered grid method as described by Virieux (1986), but with the addition of anisotropy. Figure 1 illustrates the basic structure of the network, and how seismic records are obtained from it (see also Zhang et al., 2020).

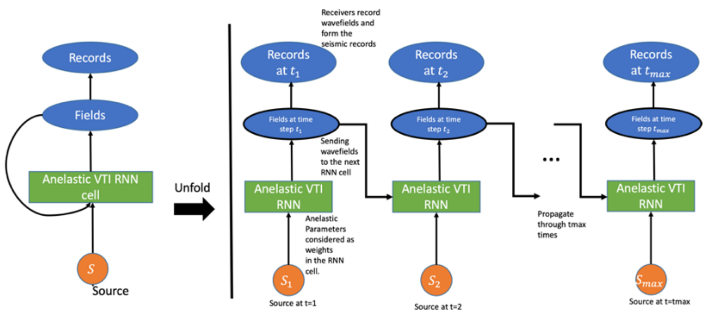

Figure 1: Anelastic RNN propagation.

Objective function

In this test, we use the following equation as the objective function:

$$
\Phi_p^{TV}(\mathbf{C}, \mathbf{QC}) = \frac{1}{2}\left\|\boldsymbol{D_{syn}}(\mathbf{C}, \mathbf{QC}) - \boldsymbol{D_{obs}}\right\|_p^p + \alpha_{1_*}^{C_*}\Theta_{TV}(C_*) + \alpha_{2_*}^{C_*}\Omega_{TV}(C_*)
$$
$$
+\alpha_{1_*}^{QC_*}\Theta_{TV}(QC_*) + \alpha_{2_*}^{QC_*}\Omega_{TV}(QC_*)\,, \tag{4}
$$

where $\alpha_{1_*}^{C_*}$, $\alpha_{2_*}^{C_*}$, $\alpha_{1_*}^{QC_*}$,$\alpha_{2_*}^{QC_*}$ are the are the values of the Lagrange multipliers. $\boldsymbol{D_{obs}}$ are the observed data. $\boldsymbol{D_{syn}}(\mathbf{C}, \mathbf{QC})$ are the synthetic data. Θ_{TV} and Ω_{TV} are functions for calculating the first-order and second-order TV regularization. We set *p* = 1, thus, the objective function is based on the l_1 norm, which is non-differentiable, but in our formulation, gradients can be calculated numerically via backpropagation along the computational graph. The wave equation based on constitutive relationship of equation 1 is not self-adjoint (Fabien-Ouellet et al., 2016), which needs a modification to use the conventional adjoint state method to perform the inversion. However, under our inversion framework, the RNN based inversion, the gradient can be given automatically by using the backpropagation method.

NUMERICAL TESTS

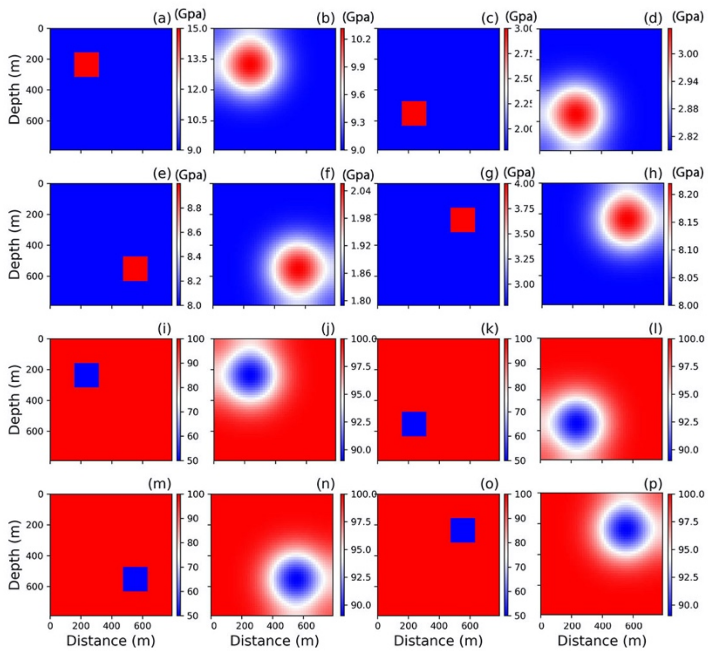

Figure 2: True and initial models for inversion. (a)-(b) True and initial C_{11}. (c)-(d) True and initial C_{13} . (e)-(f) True and initial C_{33}. (g)-(h) True and initial C_{44}. (i)-(j) True and initial QC_{11}. (k)-(l) True and initial QC_{13}. (m)-(n) True and initial QC_{33}. (o)-(p) True and initial QC_{44}.

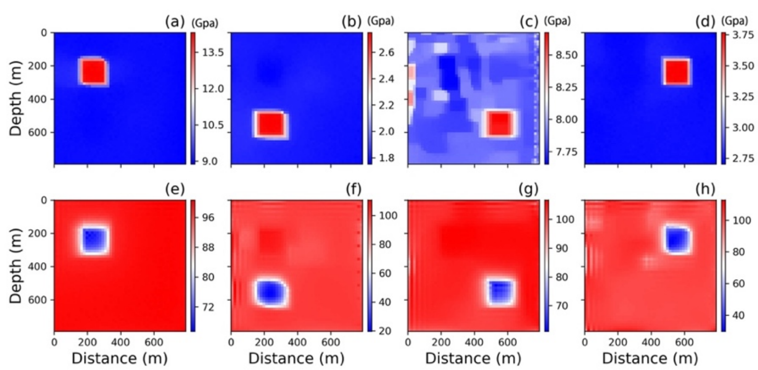

Figure 3: RNN anisotropic viscoelastic FWI with high-order total variation. (a)-(d) $C_{11}, C_{13}, C_{33}, C_{44}$ inversion results. (e)-(h) $QC_{11}, QC_{13}, QC_{33}, QC_{44}$ inversion results.

To examine our method, a simple box anomaly test is first carried out. The size of the model is 80×80, the grid cell size is dx = dz = 10m, and the source is a Ricker wavelet with a central frequency of 15Hz. The gradient based optimization Adam algorithm is used as the optimization method. The true and initial models are displayed in Figure 2 and inversion results are plotted in Figure 3. We can see that the inversion results have well recovered the box anomaly shape for the parameters and suffer few from the cross-talk between parameters, which means that the objective function based on high-order TV regulation do has the ability to mitigate cross-talk between parameters.

In order to validate the approach within more geologically complex environments, we then apply the approach to a portion of the Marmousi model. The anisotropic models are obtained by scaling the isotropic Marmousi models. In Figure 4 the results are plotted. The size of the model is 125×125, with dx = dz = 10m, and a Ricker source wavelet with central frequency 25Hz. We again employ the l_1 norm with high-order TV regularization as the objective function and optimize with the Adam algorithm. The maximum number of iterations is 100. Some error is visible in the C_{13} and C_{33} models also, which is likely the effect of parameter cross-talk, but we conclude that the l_1 objective function with TV regularization goes quite far towards mitigating the cross-talk between parameters.

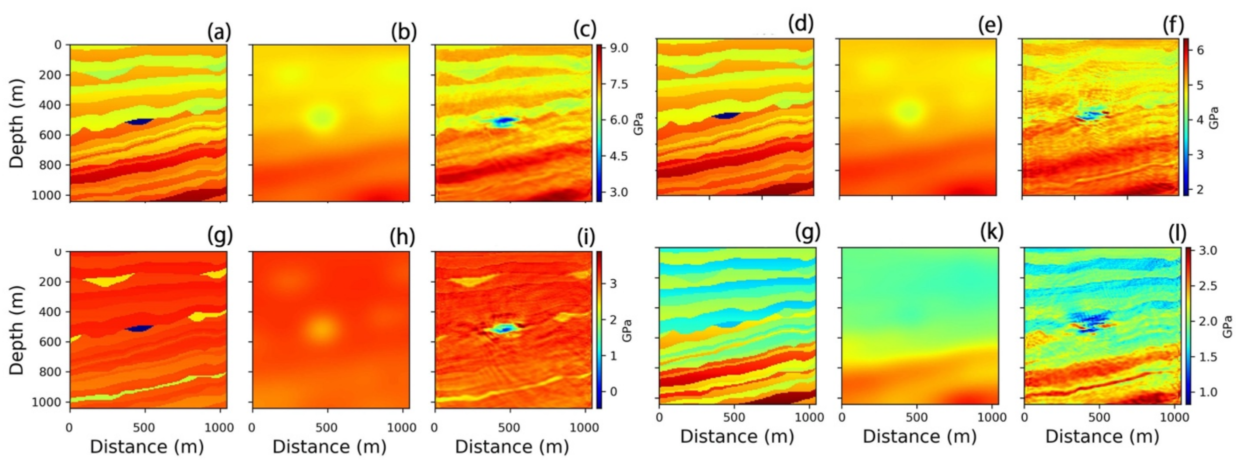

Figure 4: Cross-well data and surface data acquisition RNN viscoelastic VTI FWI with high-order total variation. (a)-(c) True, initial and inversion results for C_{11}. (d)-(f) True, initial and inversion results for C_{33}. (g)-(i) True, initial and inversion results for C_{13}. (j) -(l) True, initial and inversion results for C_{44}.

CONCLUSIONS

We formulate and implement a theory-guided anisotropic viscoelastic recurrent neural network, and train it with simulated data, which emulates full waveform inversion for eight parameters. The unique features of this RNN-FWI approach is that it can invoke objective functions that are non-differentiable, and it can straightforwardly incorporate wave operators that are non self-adjoint. It may also be of interest because of the architectures available on which to implement such networks. We set as our main challenge to find an optimization approach for which anisotropic and viscoelastic medium properties could be recovered with adequate accuracy, resolution, and while mitigating cross-talk. From numerical testing on simple synthetics, we conclude that an objective function based on the l_1 norm with high-order TV regularization is such a formulation and is an approach that should allow the benefits of the RNN-FWI to be made use of in seismic applications. Applications to field data, and more efficient HPC solutions are subjects of current research.

ACKNOWLEDGMENTS

This work was funded by the industrial sponsors of the Consortium for Research in Elastic Wave Exploration Seismology (CREWES), by the NSERC grants CRDPJ 461179-13 and CRDPJ 543578-19, and also in part by the Canada First Re- search Excellence Fund. We gratefully acknowledge continued support. The lead author was supported in this work by the China Scholarship Council.

REFERENCES

Belahi, T., S. Singh, and N. Fuji, 2016, Viscoelastic full wave- form inversion of sea bottom long offset seismic data in presence of attenuation: Presented at the 78th EAGE Conference and Exhibition 2016.

Christensen, R., 2012, Theory of viscoelasticity: an introduction: Elsevier.

Fabien-Ouellet, G., E. Gloaguen, and B. Giroux, 2016, The ad- joint state method for the viscoelastic wave equation in the velocity-stress formulation: Presented at the 78th EAGE Conference and Exhibition 2016.

———, 2017, Time-domain seismic modeling in viscoelastic media for full waveform inversion on heterogeneous computing platforms with opencl: Computers & Geosciences, 100, 142–155.

Flu ̈gge, W., 2013, Viscoelasticity: Springer Science & Business Media.

Richardson, A., 2018, Seismic full-waveform inversion using deep learning tools and techniques: arXiv preprint arXiv:1801.07232.

Robertsson, J. O., J. O. Blanch, and W. W. Symes, 1994, Viscoelastic finite-difference modeling: Geophysics, 59, 1444–1456.

Sun, J., Z. Niu, K. A. Innanen, J. Li, and D. O. Trad, 2020, A theory-guided deep-learning formulation and optimization of seismic waveform inversion: Geophysics, 85, R87–R99.

Virieux, J., 1986, P-sv wave propagation in heterogeneous me- dia: Velocity-stress finite-difference method: Geophysics, 51, 889–901.

Zhang, T., K. A. Innanen, J. Sun, and D. O. Trad, 2020, Nu- merical analysis of a deep learning formulation of multi-parameter elastic full waveform inversion, *in* SEG Techni- cal Program Expanded Abstracts 2020: Society of Exploration Geophysicists, 1531–1535.